

# Silencing KLF6 Alleviates Cigarette Smoke Extract-Induced Mitochondrial Dysfunction in Bronchial Epithelial Cells by SIRT4 Upregulation

Menghong Wan, Chen Wang, Jiamin Cui, Qing Xia, Lei Zhang 

Caoyang Community Health Service Center, Shanghai, 200063, People's Republic of China

Correspondence: Lei Zhang, Caoyang Community Health Service Center, No. 121 Lanxi Street, Putuo District, Shanghai, 200063, People's Republic of China, Email Zhanglei\_871007@163.com

**Background:** The incidence of chronic obstructive pulmonary disease (COPD) is increasing year by year. Kruppel-like factor 6 (KLF6) plays an important role in inflammatory diseases. However, the regulatory role of KLF6 in COPD has not been reported so far.

**Methods:** The viability of human bronchial epithelial cells BEAS-2B induced by cigarette smoke extract (CSE) was detected by CCK-8 assay. The protein expression of KLF6 and sirtuin 4 (SIRT4) was appraised with Western blot. RT-qPCR and Western blot were applied to examine the transfection efficacy of sh-KLF6 and Oe-KLF6. Cell apoptosis was detected using flow cytometry. The levels of inflammatory factors IL-6, TNF- $\alpha$  and IL-1 $\beta$  were assessed with ELISA assay. DCFH-DA staining was employed for the detection of ROS activity and the levels of oxidative stress markers SOD, CAT and MDA were estimated with corresponding assay kits. The mitochondrial membrane potential (MMP), adenosine triphosphate (ATP) content and Complex I activity were evaluated with JC-1 staining, ATP colorimetric/fluorometric assay kit and Complex I enzyme activity microplate assay kit. With the application of mitochondrial permeability transition pore detection kit, mPTP opening was measured. Luciferase report assay was employed to evaluate the activity of SIRT4 promoter and chromatin immunoprecipitation (ChIP) to verify the binding ability of KLF6 and SIRT4 promoter.

**Results:** KLF6 expression was significantly elevated in CSE-induced cells. KLF6 was confirmed to suppress SIRT4 transcription. Interference with KLF6 expression significantly inhibited cell viability damage, cell apoptosis, inflammatory response, oxidative stress and mitochondrial dysfunction in CSE-induced BEAS-2B cells, which were all reversed by SIRT4 overexpression.

**Conclusion:** Silencing KLF6 alleviated CSE-induced mitochondrial dysfunction in bronchial epithelial cells by SIRT4 upregulation.

**Keywords:** KLF6, SIRT4, COPD, CSE, mitochondrial dysfunction

## Introduction

Respiratory diseases, which are critical contributors to death and disability worldwide, have been an emerging public health concern and bring a heavy burden to patients as well as their caregivers.<sup>1</sup> As a preventable and treatable disease, chronic obstructive pulmonary disease (COPD) is characterized by recurrent respiratory symptoms and irreversible airflow restriction, becoming the fourth leading driver of death.<sup>2</sup> As is known to all, cigarette smoke is a prominent contributor to COPD.<sup>3</sup> It is believed that the long-term exposure of airway epithelial cells to cigarette smoke can bring about inflammation, oxidative damage and protease imbalance.<sup>4</sup> In addition, inflammation and imbalance of antioxidant defense systems are main triggers for the pathogenesis of COPD, and are also prospective targets for the treatment of COPD.<sup>5,6</sup> Therefore, it is of great significance to search for COPD biomarkers and explore the disease mechanism.

Kruppel-like factor (KLF) is a family of transcription factors with zinc finger structure, which plays a variety of biological roles in regulating growth, proliferation, differentiation, development, inflammation and apoptosis.<sup>7</sup> KLF6, which is also known as transcription factor ZF9, belongs to the KLF family.<sup>8</sup> A previous study has shown that the inhibition of KLF6 can reduce the inflammation and apoptosis of type II alveolar epithelial cells in acute lung injury.<sup>9</sup>

Additionally, the trans-activation of iNOS gene by KLF6 can promote apoptosis during respiratory syncytial virus infection.<sup>10</sup> In addition, study has analyzed the differential genes of samples from patients with acute exacerbation of COPD and stable COPD and found that KLF6 is up-regulated.<sup>11</sup>

Sirtuins, a class of histone deacetylases, play important mediated function in a diverse range of pathophysiological processes, such as inflammation, cell apoptosis, cell proliferation, cell senescence and oxidative stress.<sup>12,13</sup> SIRT4, which is a member of the Sirtuin family, has been evidenced to possess anti-inflammation and anti-oxidant properties.<sup>14</sup> Additionally, a previous study has corroborated that SIRT4 expression was downregulated in cigarette smoke extract (CSE)-challenged human pulmonary microvascular endothelial cells (HPMECs) in COPD.<sup>15</sup> Intriguingly, JASPAR database (<http://jaspar.genereg.net/>) predicted that KLF6 could bind to SIRT4 promoter. However, the mechanism of KLF6 in COPD associated with SIRT4 remains obscure.

In summary, this study intended to explore the regulatory role of KLF6 in the occurrence and development of COPD as well as to discuss the hidden reaction mechanism, aiming to shed novel insights into the development of prospective therapeutic targets for COPD treatment.

## Materials and Methods

### Database

JASPAR database was used to predict the binding sites of transcription factor KLF6 and SIRT4 promoter.<sup>16</sup>

### CSE Preparation

CSE was prepared as previously described.<sup>17</sup> In brief, 400 mL of cigarette smoke from commercial Da Qianmen cigarettes (containing 2.5 mg of nicotine and 12 mg of tar per cigarette) was drawn into a modified 50 mL syringe apparatus. Following the filter of large particles and bacteria with a 0.22  $\mu\text{m}$  filter, the smoke mixed with 20 mL serum-free RPMI1640 was defined to be 100% CSE. 100% CSE was diluted with RPMI1640 medium to indicated concentration and used within 15 min after preparation.

### Cell Culture

Human bronchial epithelial cell line BEAS-2B was purchased from the Shanghai Institute of Cell Biology, Chinese Academy of Sciences (Shanghai, China). All cells were planted ( $5 \times 10^4$  cells/mL) in 6-well plates and cultured in RPMI1640 medium supplemented with 10% FBS (Sigma) and 1% penicillin/streptomycin (Sigma) in a humidified incubator containing 5%  $\text{CO}_2$  at 37°C. The culture medium was changed every 48 h. For CSE treatment, BEAS-2B cells were maintained in medium without FBS with CSE 1, 2 and 5% for 24 h.<sup>17</sup>

### Cell Transfection

For transfection, short hairpin RNA specific to KLF6 (sh-KLF6#1 and sh-KLF6#2), short hairpin RNA targeting SIRT4 (sh-SIRT4#1 and sh-SIRT4#2), the corresponding BEAS-2B cells control plasmids (sh-NC), pc-DNA3.1 vectors containing the complete sequence of KLF6 (Oe-KLF6) and the empty vector (Oe-NC) were synthesized by GenePharma (Shanghai, China). With the employment of Lipofectamine 2000 (Invitrogen, Thermo Fisher Scientific, Inc.), 100 nM recombinants were transfected into BEAS-2B cells according to the manufacturer's instructions for 48 h at 37°C. After 48 h, cells were collected for subsequent experiments.

### Cell Viability Assay

Cell Counting Kit-8 (CCK-8, Beyotime Biotechnology, China) was adopted to estimate BEAS-2B cell viability following the operating instructions. Briefly, BEAS-2B cells were harvested in the logarithmic growth phase and injected into 96-well plates at a density of  $3 \times 10^4$  cells/well, following which was the cultivation at 37°C for 24 h. After that, BEAS-2B cells were exposed to CCK-8 solution (10  $\mu\text{L}$ ) for additional 2 h at 37°C. The absorbance value run at 450 nm was analyzed with a microplate reader (Promega, WI, USA).

## Cell Apoptosis

Cell apoptosis was detected using Annexin V-FITC/PI Apoptosis Detection Kit (KGA105, KeyGEN, Jiangsu, China) following manufacturer's instructions. Following the rinse with pre-cold PBS and the resuspension in 100  $\mu$ L binding buffer, BEAS-2B cells were incubated with 2  $\mu$ L Annexin-V-FITC (20  $\mu$ g/mL, Sigma) on ice in the dark for 15 min. Subsequently, BEAS-2B cells were stained with 5  $\mu$ L of Annexin V-FITC and 5  $\mu$ L propidium iodide (PI, BD Biosciences) in 1 mL of binding buffer for 15 min in the dark. Cells were quantified with a flow cytometer (BD Biosciences, NY, USA).

## Western Blot Analysis

Samples extracted from BEAS-2B cells were homogenized in lysis buffer (Beyotime Institute of Biotechnology, Jiangsu, China). The concentration of proteins was quantified by virtue of bicinchoninic acid (BCA) protein assay kits (Thermo Fisher Scientific Inc.) according to the operating manual provided by manufacturers. Following the separation with 8% SDS-PAGE, proteins (20  $\mu$ g per lane) were loaded onto PVDF membranes (BioRad, Hercules, CA). Blocked with 5% BSA, membranes were immunoblotted with primary antibodies against KLF6 (cat. no. 14716-1-AP; 1:1000, Proteintech), SIRT4 (cat. no. 66543-1-Ig; 1:20000, Proteintech), and GAPDH (cat. no. 60004-1-Ig; 1:50000, proteintech) at 4°C overnight and horseradish peroxidase-labeled goat anti-rabbit secondary antibody (cat. no. HRP-11449; 1:5000, Proteintech) for 2 h at room temperature. Protein bands were visualized by enhanced chemiluminescent (ECL) kit (Bio-Rad Laboratories, Inc, CA, USA), and the relative density of each band was calculated with Image J software (Version 1.49; National Institutes of Health). GAPDH served as a control to standardize the results.

## Reverse Transcription-Quantitative PCR (RT-qPCR)

Total RNA was extracted from sample BEAS-2B cells by means of Trizol reagent (Gibco, Grand Island, NY, USA) according to the protocol. With the application of a commercial RevertAid™ cDNA Synthesis kit (Bio-Rad), RNA was reverse transcribed into cDNA in light of the operating manual. Afterwards, the amplification of templates was implemented on the 7500 Fast Real-time PCR system by means of SYBR Green PCR Master Mix (Takara) in light of standard protocol. The relative mRNA expression level was valued by  $2^{-\Delta\Delta C_t}$  method<sup>18</sup> with GAPDH acting as an endogenous control. The primer sequences were listed as follows: KLF6 forward primer: 5'-TCCCACGGCCAAGTTTACCT-3', reverse primer: 5'-AAGGCTT TTCTCCTGGCTTCCC-3'; SIRT4 forward primer: 5'-CTCGAAAGCCTCCATTGGGT-3', reverse primer: 5'-GGCCAGC CTACGAAGTTTCT-3'; GAPDH forward primer: 5'-TGTGGGCATCAATGGATTGG-3', reverse primer: 5'-ACACCAT GTATTCCGGGTCAAT-3'.

## Enzyme-Linked Immunosorbent Assay (ELISA) Assay

The levels of tumor necrosis factor- $\alpha$  (TNF- $\alpha$ ), interleukin 1beta (IL-1 $\beta$ ) and interleukin-6 (IL-6) in the supernatants of CSE-induced BEAS-2B cells were appraised with TNF- $\alpha$  (cat. no. PT518, Beyotime Institute of Biotechnology), IL-1 $\beta$  (cat. no. PI305, Beyotime Institute of Biotechnology) and IL-6 (cat. no. PI330, Beyotime Institute of Biotechnology) according to the manufacturer's instructions.

## Measurement of ATP

The content of adenosine triphosphate (ATP) in mitochondria was appraised with the adoption of an ATP Colorimetric/Fluorometric Assay Kit (Biovision, Milpitas, CA, USA) according to the manufacturer's instructions. In brief, the lysis of BEAS-2B cells ( $1 \times 10^5$ ) with probe sonication was conducted in 100  $\mu$ L of ATP assay buffer on ice, following which was the transfer of lysates to a 96-well microplate. Subsequently, the samples were exposed to Reaction Mix for 30 min at room temperature, and the absorbance value run at 570 nm was recorded utilizing a VICTOR X3 Multilabel Plate Reader (PerkinElmer, Waltham, MA, USA).

## Complex I Activity Assay

By means of Complex I Enzyme Activity Microplate Assay Kit (Abcam, Cambridge, UK), the activity of Complex I was estimated in light of standard protocol. In brief, the lysis of BEAS-2B cells ( $1 \times 10^5$ ) was conducted with detergent

solution on ice. Following centrifugation, the protein concentration of the collected supernatant was normalized.<sup>19</sup> After that, the sample cells were incubated at room temperature for 3 h and then probed with assay solution for 30 min at room temperature. With the application of a VICTOR X3 Multilabel Plate Reader (PerkinElmer, Waltham, MA, USA), the absorbance was measured at 450 nm.

### Dichloro-Dihydro-Fluorescein Diacetate (DCFH-DA) Staining

The activity of reactive oxygen species (ROS) was assessed by means of ROS assay kits (cat. no. S0033S, Beyotime Institute of Biotechnology). Briefly, BEAS-2B cells were stained by DCFH-DA probe (10  $\mu\text{mol/l}$ ) for 20 min at 37 °C. After the wash with PBS, the fluorescence intensity was measured by a confocal laser microscopy (Leica, Germany) with excitation and emission at 488 nm and 522 nm, respectively.

### Detection of Oxidative Stress Related Indexes

The activities of superoxide dismutase (SOD), malondialdehyde (MDA) and catalase (CAT) were, respectively, assessed by SOD assay kits (cat. no. S0109, Beyotime Institute of Biotechnology), MDA assay kits (cat. no. S0131S, Beyotime Institute of Biotechnology) and CAT assay kits (cat. no. S0082, Beyotime Biotechnology) strictly in accordance with the recommended specifications.

### 5.5',6.6'-Tetrachloro-1,1',3,3'-Tetraethylbenzimidazolocarbo- Cyanine Iodide (JC-1) Staining

The mitochondrial membrane potential (MMP) was detected with JC-1 staining kit (Beyotime). BEAS-2B cells were stained by JC-1 (10  $\mu\text{g/mL}$ ) at 37 °C for 20 min. MMP was visualized by fluorescence microscopy (Olympus, Tokyo, Japan). Red fluorescence represented aggregates. Green fluorescence represented the monomeric form of JC-1.

### Mitochondrial Permeability Transition Pore (mPTP) Opening Evaluation

The mPTP opening was measured by the Mitochondrial Permeability Transition Pore Detection Kit (GMS10095.1, GENMED scientifics Inc., MA, USA) and was determined by monitoring the decrease in light scattering at 545 nm with a confocal laser microscopy (Leica, Germany).

### Luciferase Reporter Assay

JASPAR database predicted the binding sites of transcription factor KLF6 and SIRT4 promoter. Through the implementation of luciferase reporter assay on the Luciferase Reporter System (Promega), the interaction between KLF6 and SIRT4 promoter was verified. Wild-type (WT) and mutant (MUT) SIRT4 promoter were cloned into the pGL3 Basic vector (Promega Corporation). BEAS-2B cells were inoculated into 24-well plates for 24 h at 37°C and then transfected with above plasmids and pcDNA3.1 plasmid overexpressing KLF6 (Oe-KLF6) and the empty plasmid pcDNA3.0 (Oe-NC) using Lipofectamine 2000 reagent (Thermo Fisher Scientific Inc.) at 37°C according to the operating manual. 48 h post-transfection, BEAS-2B cells were lysed, and luciferase reporter activity was measured using the Luciferase Reporter system (Promega) with Firefly luciferase values normalized to Renilla luciferase values.

### Chromatin Immunoprecipitation (ChIP)

For ChIP, commercially available kits (Beyotime Institute of Biotechnology) were applied. In brief, BEAS-2B cells ( $1 \times 10^6$ ) were exposed to 1% formaldehyde at 37°C for 10 min to cross-link the target protein with the corresponding genomic DNA. Following the centrifugation at  $13,000 \times g$  for 10 min at 4°C, BEAS-2B cells were washed with pre-chilled PBS twice. For the obtaining of 200–500 bp fragments, a high intensity ultrasonic processor (Cole-Parmer) was employed to shear the genomic DNA on ice. An equal amount of chromatin was immunoprecipitated at 4°C overnight. ChIP was implemented with 2  $\mu\text{g}$  anti-KLF6 and total chromatin was used as the input. Immunoprecipitated products were collected after the incubation with magnetic beads coupled with anti-rabbit IgG. The precipitated chromatin DNA was collected and analyzed by PCR.

## Statistical Analysis

All experiments were replicated for three times. All experimental data were analyzed with GraphPad Prism 8.0 software (GraphPad Software, Inc.) and presented as means  $\pm$  standard deviation (SD). For the demonstration of comparisons between two groups, Student's *t*-test was employed, while one-way ANOVA with Tukey's post hoc test was used to exhibit differences among multiple groups. A *P* value  $<0.05$  was supposed to be statistically significant.

## Results

### Inhibition of KLF6 Increased the Viability of CSE-Induced BEAS-2B Cells

To simulate CSE-induced injury, BEAS-2B cells were treated with varying concentrations of CSE (1%, 2% and 5%) and CCK8 assay was conducted to detect cell viability. The results showed that cell viability was significantly decreased by CSE induction in a concentration-dependent manner when compared with the Control group (Figure 1A). The protein expression of KLF6 in CSE-induced BEAS-2B cells was assessed with Western blot, and it was discovered that KLF6 expression in BEAS-2B cells was concentration-dependently increased by CSE induction compared with the Control group (Figure 1B). It was noted that 5% CSE has the most significant effect, in view of this, 5% CSE was selected for subsequent experiments. To downregulate KLF6 expression, sh-KLF6 was transfected into BEAS-2B cells, and the transfection efficacy was examined with RT-qPCR and Western blot. Compared with the sh-NC group, the mRNA and protein expressions of KLF6 were markedly decreased after the transfection with sh-KLF6. Evidently, the transfection efficacy of sh-KLF6#2 was more significant, so we selected sh-KLF6#2 for follow-up experiments (Figure 1C). The cells were divided into Control group (BEAS-2B cells without CSE induction), CSE group (BEAS-2B cells were induced by

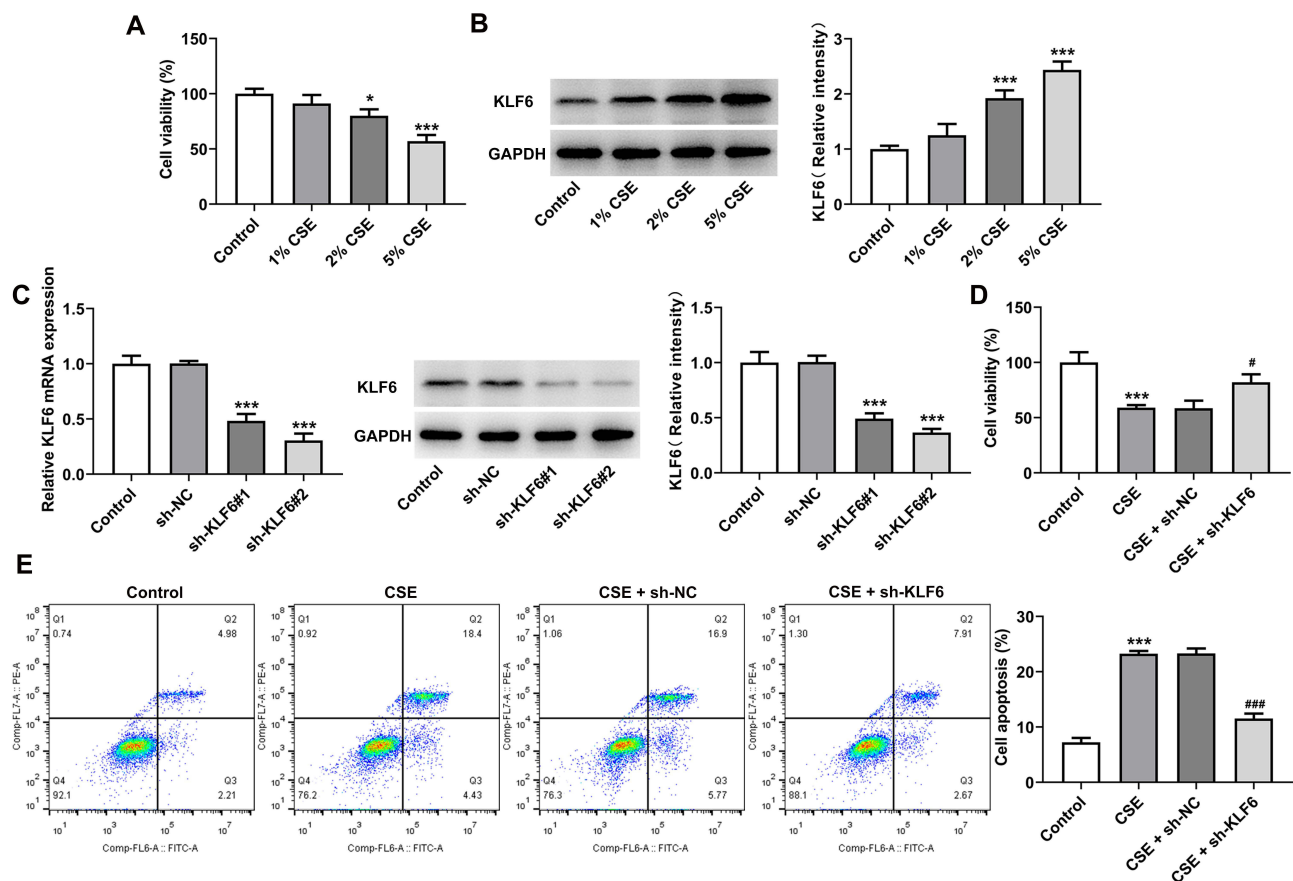


**Figure 1** Inhibition of KLF6 increased the viability of CSE-induced BEAS-2B cells. (A) Following the induction with 1%, 2% and 5% of CSE, CCK8 assay was used to detect cell viability. \**P* $<0.05$ , \*\*\**P* $<0.001$  vs Control. (B) Western blot was used to detect the expression of KLF6 in CSE-induced BEAS-2B cells. (C) The transfection efficacy of sh-KLF6 was detected using RT-qPCR and Western blot. \*\*\**P* $<0.001$  vs sh-NC. (D) CCK8 assay was used to detect cell viability. (E) Flow cytometry was used to detect cell apoptosis. \*\*\**P* $<0.001$  vs Control; #*P* $<0.05$ , ###*P* $<0.001$  vs CSE+sh-NC.

5% CSE), CSE + sh-NC group (BEAS-2B cells were induced by 5% CSE and transfected with sh-NC), and CSE + sh-KLF6 group (BEAS-2B cells were induced by 5% CSE and transfected with sh-RNA targeting KLF6). The effects of KLF6 silence on BEAS-2B cell viability and apoptosis were investigated through the implementation of CCK8 assay and flow cytometry. As Figure 1D demonstrated, a significant increase in cell viability can be observed in CSE + sh-KLF6 group compared with the CSE + sh-NC group. Flow cytometry showed that cell apoptosis was significantly facilitated after CSE induction by contrast with the Control group, which was then inhibited by KLF6 interference (Figure 1E).

## Inhibition of KLF6 Alleviates Inflammation and Oxidative Stress in CSE-Induced BEAS-2B Cells

To explore the effects of KLF6 silence on inflammation in CSE-induced BEAS-2B cells, the levels of inflammatory cytokines were detected by ELISA assay. The results showed that the expressions of IL-6, TNF- $\alpha$  and IL-1 $\beta$  in the CSE group were significantly increased compared with those in Control group. Compared with CSE+sh-NC group, the levels of these inflammatory cytokines in CSE + sh-KLF6 group were significantly decreased (Figure 2A). DCFH-DA staining was used to detect ROS level in BEAS-2B cells, and the results showed that the activity of ROS in BEAS-2B cells was significantly increased after CSE induction in comparison with the Control group. Compared with the CSE + sh-NC group, KLF6 depletion reduced ROS level (Figure 2B). The activities of oxidative stress-related indicators SOD, CAT and MDA were detected by relevant kits. Compared with the Control group, the activities of SOD and CAT were

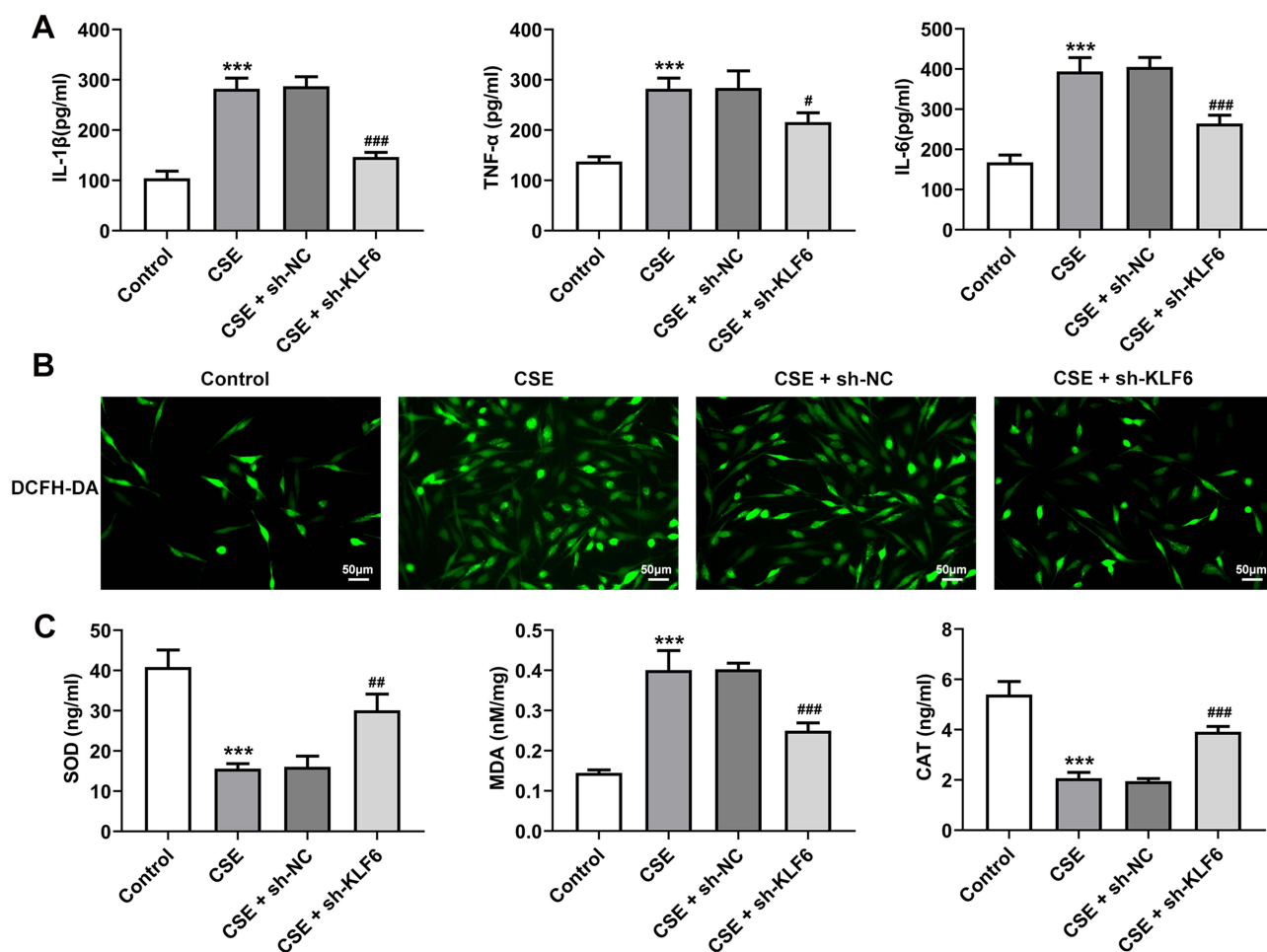


**Figure 2** Inhibition of KLF6 alleviates inflammation and oxidative stress in CSE-induced BEAS-2B cells. (A). The levels of inflammatory cytokines IL-6, TNF- $\alpha$  and IL-1 $\beta$  were detected by ELISA. (B). DCFH-DA staining was used to detect ROS level in BEAS-2B cells. (C) The levels of oxidative stress-related indicators SOD, CAT and MDA were detected by relevant kits. \*\*\* $P$ <0.001 vs Control; # $P$ <0.05, ### $P$ <0.01, #### $P$ <0.001 vs CSE+sh-NC.

decreased and MDA activity was increased in CSE group, which were then all reversed after depleting KLF6 expression (Figure 2C).

### Inhibition of KLF6 Inhibits Mitochondrial Dysfunction in CSE-Induced BEAS-2B Cells

Mitochondrial dysfunction is a critical determinant in the pathogenesis of COPD. In order to figure out the effects of KLF6 silence on mitochondrial dysfunction in CSE-induced BEAS-2B cells, the alterations of MMP were initially assessed with JC-1 staining. Compared with Control group, CSE induction decreased JC-1 aggregates and increased JC-1 monomers in BEAS-2B cells. Compared with the CSE + sh-NC group, JC-1 aggregates were increased, and JC-1 monomers were decreased in CSE + sh-KLF6 group (Figure 3A). The production of ATP by mitochondria ensures the supply of cellular energy. With the application of ATP assay kit, the production of ATP was measured and the results showed that CSE stimulation conspicuously reduced ATP level compared with the Control group, which was then increased by sh-KLF6 (Figure 3B). Complex I activity was detected by corresponding assay kit, and it was found that the decreased Complex I activity in BEAS-2B cells due to CSE induction was partially increased by KLF6 depletion when compared with the CSE + sh-NC group (Figure 3C). As Figure 3D demonstrated, mPTP was increased in the CSE group by contrast with the Control group. Compared with the CSE+sh-NC group, the mPTP in CSE + sh-KLF6 group was decreased.

### KLF6 Inhibits SIRT4 Transcription

The JASPAR website was used to predict the binding sites of transcription factor KLF6 and SIRT4 promoter (Figure 4A). To explore the protein expression of SIRT4 in CSE-induced BEAS-2B cells, Western blot was conducted, and the results exhibited that SIRT4 expression was significantly decreased by CSE induction compared with the Control group (Figure 4B). KLF6 overexpression plasmid was constructed, and its transfection efficiency was detected by RT-qPCR and Western blot. As Figure 4C depicted, the mRNA and protein expressions of KLF6 were markedly increased after the transfection with Oe-KLF6 in comparison with the Oe-NC group. Results obtained from luciferase and CHIP experiments demonstrated the binding ability between KLF6 and SIRT4 (Figure 4D and E). In addition, it was also found that KLF6 silence significantly promoted the expression of SIRT4 in CSE-induced BEAS-2B cells (Figure 4F). Moreover, the decreased SIRT4 in CSE-induced BEAS-2B cells was further reduced after overexpressing KLF6 (Figure 4G). Evidently, KLF6 could negatively regulate SIRT4 expression in BEAS-2B cells with CSE induction.

### Inhibition of KLF6 Enhances the Viability of CSE-Induced BEAS-2B Cells Through SIRT4 Upregulation

To downregulate SIRT4 expression, sh-SIRT4 was transfected into BEAS-2B cells, and the transfection efficacy was examined with RT-qPCR and Western blot. Compared with the sh-NC group, the mRNA and protein expressions of SIRT4 was remarkably decreased (Figure 5A). sh-SIRT4#2 was selected for subsequent experiments because of its prominent transfection efficacy. Then, all cells were divided into five groups: Control, CSE, CSE+sh-KLF6, CSE+sh-KLF6+sh-NC (BEAS-2B cells were induced by 5% CSE and co-transfected with sh-KLF6 and sh-NC), and CSE+sh-KLF6+sh-SIRT4 groups (BEAS-2B cells were induced by 5% CSE and co-transfected with sh-KLF6 and sh-SIRT4). Results obtained from flow cytometry showed that compared with CSE + sh-KLF6 + sh-NC group, the apoptosis in CSE+ sh-KLF6 + sh-SIRT4 group was significantly increased (Figure 5B).

### Inhibition of KLF6 Alleviates Inflammation and Oxidative Stress in CSE-Induced BEAS-2B Cells Through SIRT4 Upregulation

The levels of inflammatory cytokines were measured with ELISA, and it was found that compared with CSE+sh-KLF6 +sh-NC group, the expressions of IL-6, TNF- $\alpha$  and IL-1 $\beta$  in CSE+sh-KLF6+sh-SIRT4 group were significantly increased (Figure 6A). Compared with CSE+sh-KLF6+sh-NC group, ROS and MDA levels in CSE+sh-KLF6+sh-SIRT4 group were increased, while SOD and CAT levels were decreased (Figure 6B and C).

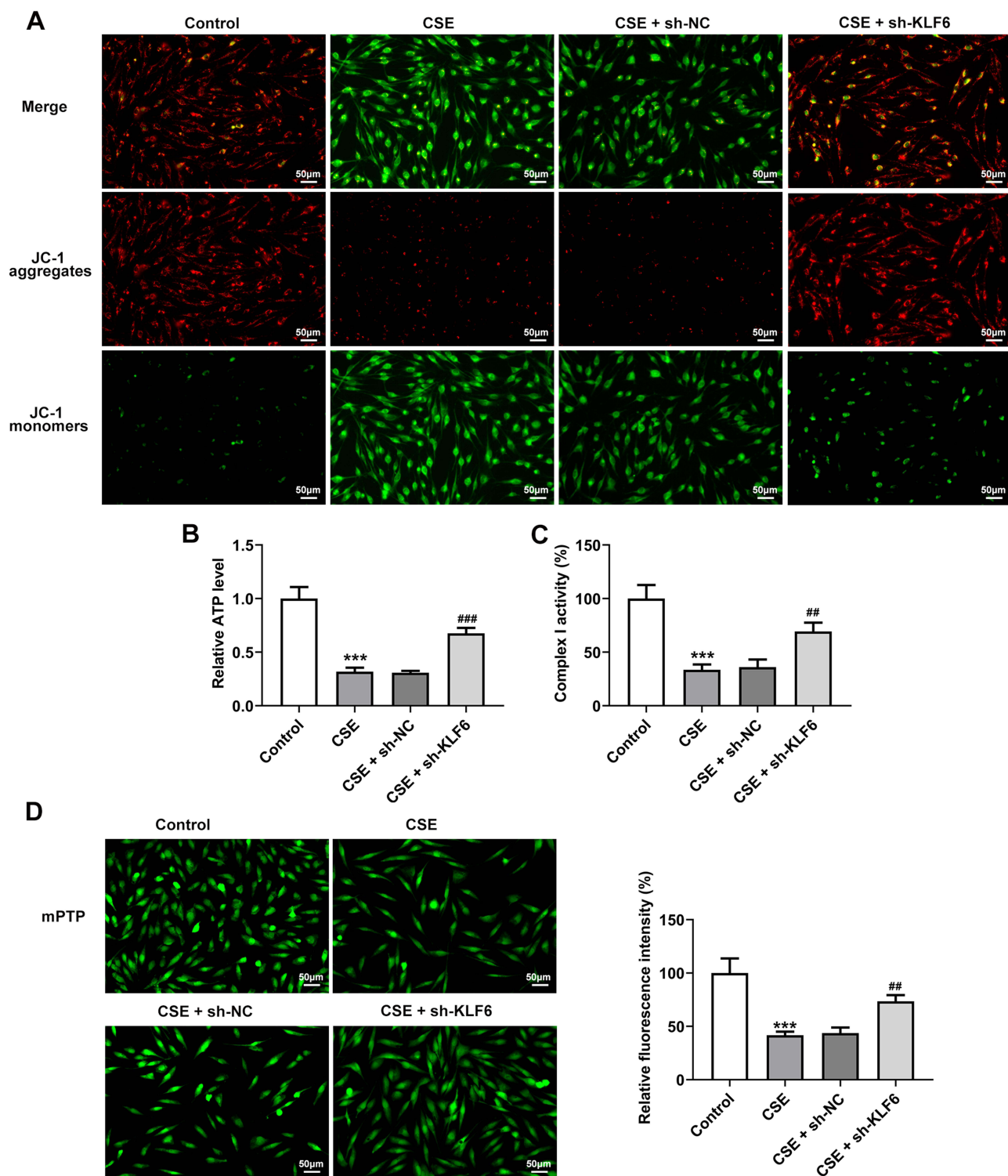


**Figure 3** Inhibition of KLF6 inhibits mitochondrial dysfunction in CSE-induced BEAS-2B cells. (A) The MMP was detected by JC-1 fluorescent probe. (B) ATP content was measured with an ATP kit. (C) Complex I activity was detected by the kit. (D) The mPTP opening was tested by corresponding kit. \*\*\* $P < 0.001$  vs Control; ### $P < 0.01$ , #### $P < 0.001$  vs CSE+sh-NC.

## Inhibition of KLF6 Alleviates Mitochondrial Dysfunction in CSE-Induced BEAS-2B Cells Through SIRT4 Upregulation

Compared with the CSE+sh-KLF6+sh-NC group, JC-1 aggregates were decreased, and JC-1 monomers were increased in the CSE+sh-KLF6+sh-SIRT4 group (Figure 7A). ATP and Complex I activities were detected by corresponding assay

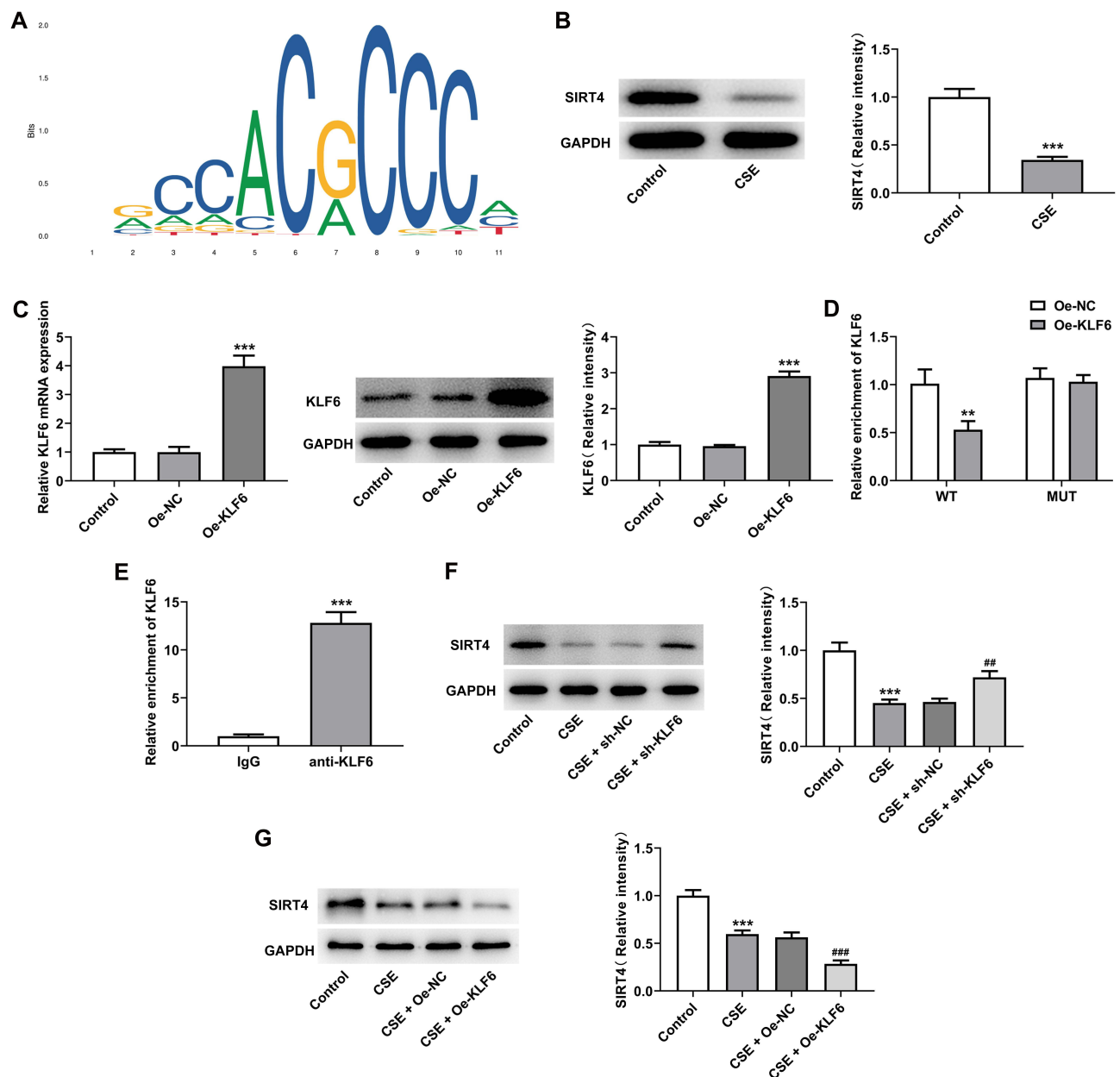


**Figure 4** KLF6 inhibits SIRT4 transcription. **(A)**. The JASPAR website predicts the binding sites between transcription factor KLF6 and SIRT4 promoter. **(B)**. Western blot was used to detect the expression of SIRT4 in CSE-induced BEAS-2B cells.  $***P<0.001$  vs Control. **(C)**. KLF6 overexpression plasmid was constructed, and its transfection efficiency was detected by RT-qPCR and Western blot.  $***P<0.001$  vs Oe-NC. **(D)**. The activity of SIRT4 promoter was detected using luciferase report assay.  $**P<0.01$  vs Oe-NC. **(E)**. ChIP assay was used to detect the binding ability of KLF6 with SIRT4.  $***P<0.001$  vs IgG. **(F)**. Western blot was used to detect the expression of SIRT4. **(G)**. Western blot was used to detect the expression of SIRT4 in CSE-induced BEAS-2B cells transfected with Oe-KLF6.  $***P<0.001$  vs Control;  $##P<0.01$  and  $###P<0.001$  vs CSE+sh-NC.

kits, and the results showed that ATP content and Complex I activity were decreased in CSE+sh-KLF6+sh-SIRT4 group compared with CSE+sh-KLF6+sh-NC group (Figure 7B and C). Additionally, the mPTP test results showed that mPTP was increased in CSE+sh-KLF6+sh-SIRT4 group compared with CSE+ sh-KLF6+sh-NC group (Figure 7D).

## Discussion

Smoke from cigarette is a harmful mixture of more than 5,000 chemicals and a large number of free radicals, which is produced by the combustion, thermal decomposition and concentration of tobacco under aerobic and anoxic conditions.<sup>20</sup> When cigarette smoke is inhaled into the lungs, it first causes oxidative stress and inflammation in the lungs, activates the

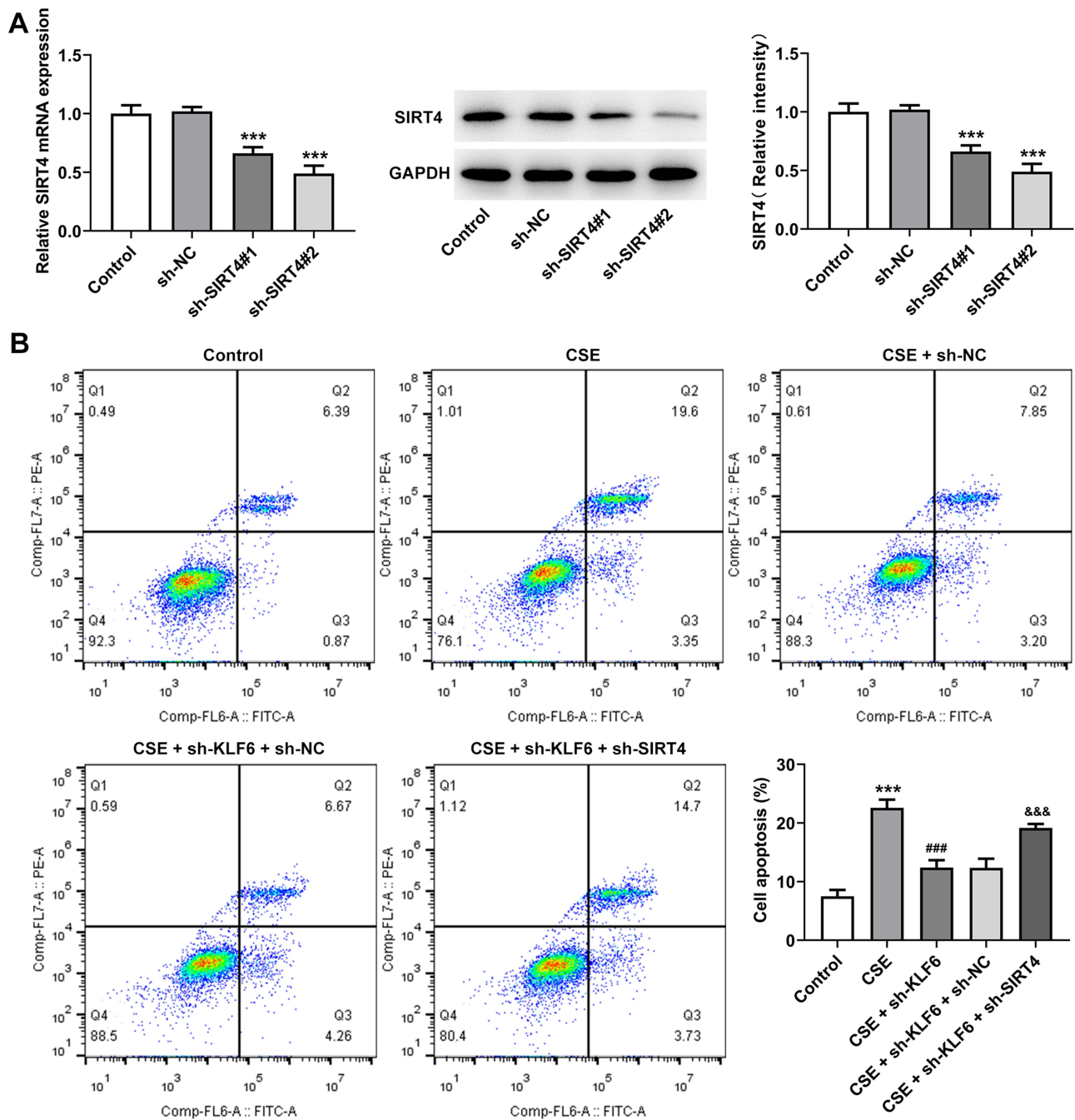


**Figure 5** Inhibition of KLF6 enhances CSE-induced BEAS-2B cell viability through SIRT4 upregulation. **(A)** The transfection efficiency of sh-SIRT4 was detected by RT-qPCR and Western blot. \*\*\* $P < 0.001$  vs sh-NC. **(B)** Flow cytometry was used to detect cell apoptosis. \*\*\* $P < 0.001$  vs Control; #### $P < 0.001$  vs CSE; &&& $P < 0.001$  vs CSE+sh-KLF6+sh-NC.

inflammatory signaling pathway of airway epithelial cells and alveolar macrophages, recruits more immune cells to the lungs, secretes a large number of inflammatory factors and proteases and then further amplifies inflammation, accompanied by imbalance between oxidative stress and proteinase-antiprotease.<sup>21</sup> Besides, cigarette smoke has been elucidated to be a predominant source of ROS, and excessive ROS production contributes to oxidative stress, thereby triggering the development of pathological changes in the lungs of COPD patients<sup>22</sup> In addition, CSE can activate molecules involved in the cell cycle and mediate cell apoptosis.<sup>23</sup> Moreover, the abnormal inflammation in the lungs

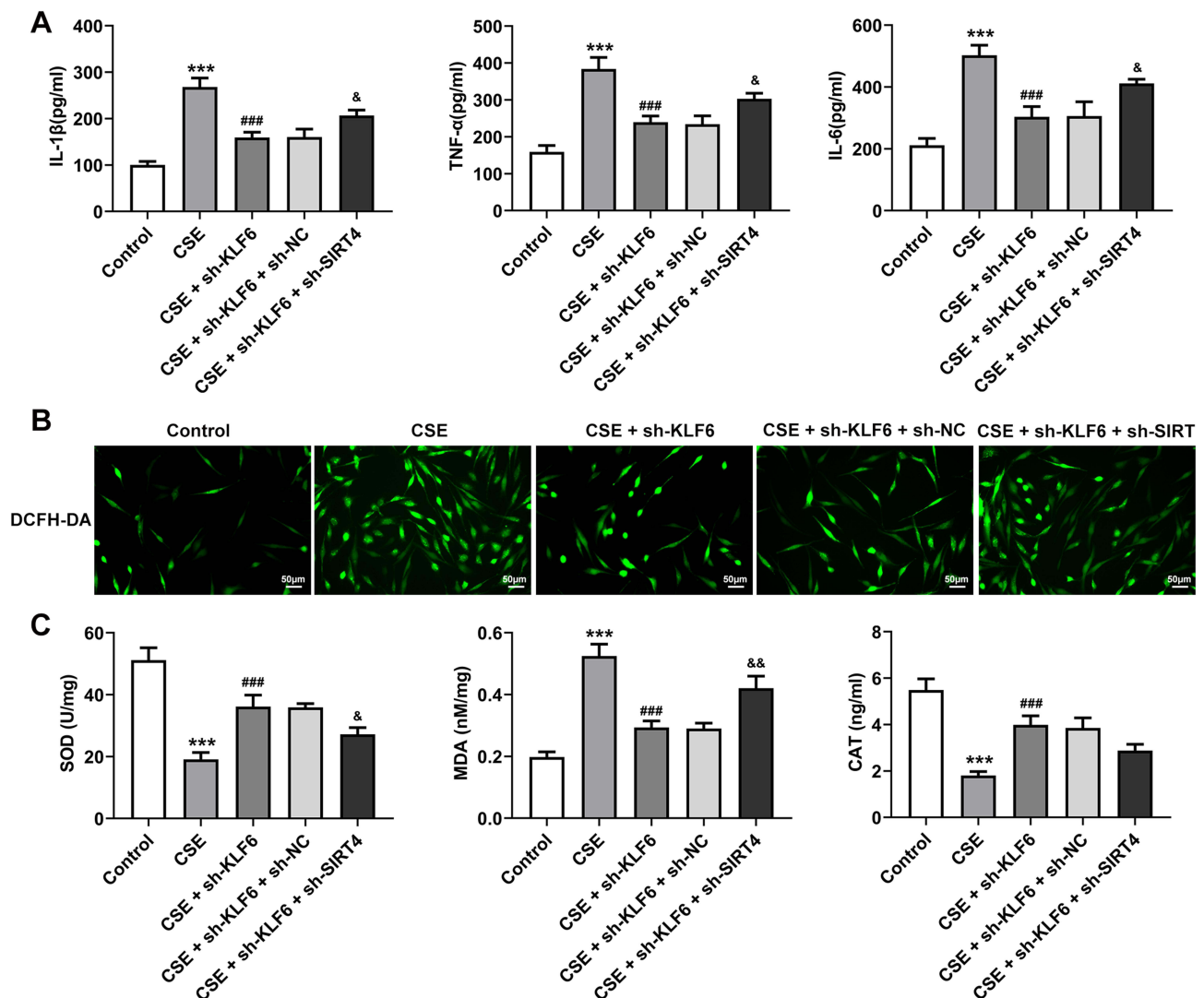


**Figure 6** Inhibition of KLF6 alleviates inflammation and oxidative stress in CSE-induced BEAS-2B cells through SIRT4 upregulation. (A). The levels of inflammatory cytokines IL-6, TNF- $\alpha$  and IL-1 $\beta$  were detected by ELISA. (B). DCFH-DA staining was used to detect ROS level. (C). The levels of oxidative stress related indicators SOD, CAT and MDA were detected by relevant kits. \*\*\* $P < 0.001$  vs Control; #### $P < 0.001$  vs CSE; & $P < 0.05$ , && $P < 0.01$  vs CSE+sh-KLF6+sh-NC.

caused by the inhalation of cigarette smoke has close association with COPD.<sup>24</sup> Results of the present study demonstrated that CSE induction promoted the apoptosis, inflammation and oxidative stress in BEAS-2B cells.

In our experiments, we found that the expression of KLF6 in cells was significantly increased with the increase of CSE concentration. Study has shown that the expression of KLF6 is significantly up-regulated in COPD exacerbations.<sup>11</sup> KLF6 overexpression has been proved to promote cell apoptosis and facilitate the release of pro-inflammatory cytokines in LPS-induced periodontal ligament cells.<sup>25</sup> Furthermore, Sun et al have clarified that the depletion of KLF6 could prevent oxidative stress in intracerebral hemorrhage rats.<sup>26</sup> However, the role of KLF6 in inflammation, apoptosis and oxidative stress in COPD has not been reported yet. In the present study, KLF6 interference was discovered to inhibit cellular inflammation, repress cell apoptosis and suppress oxidative stress in CSE-induced BEAS-2B cells.

Mitochondria have the function of synthesizing ATP to provide energy for cells.<sup>27</sup> Therefore, mitochondria are important organelles involved in cell energy metabolism, signal transduction and apoptosis. If mitochondrial function is abnormal, it will lead to the changes in the functional state of cells and affect the occurrence and prognosis of diseases.<sup>28</sup> Numerous studies have shown that mitochondrial dysfunction exists in COPD patients.<sup>29,30</sup> Chronic airway inflammation in COPD caused by common smoking, ROS produced by smoke and endogenous ROS produced by mitochondrial

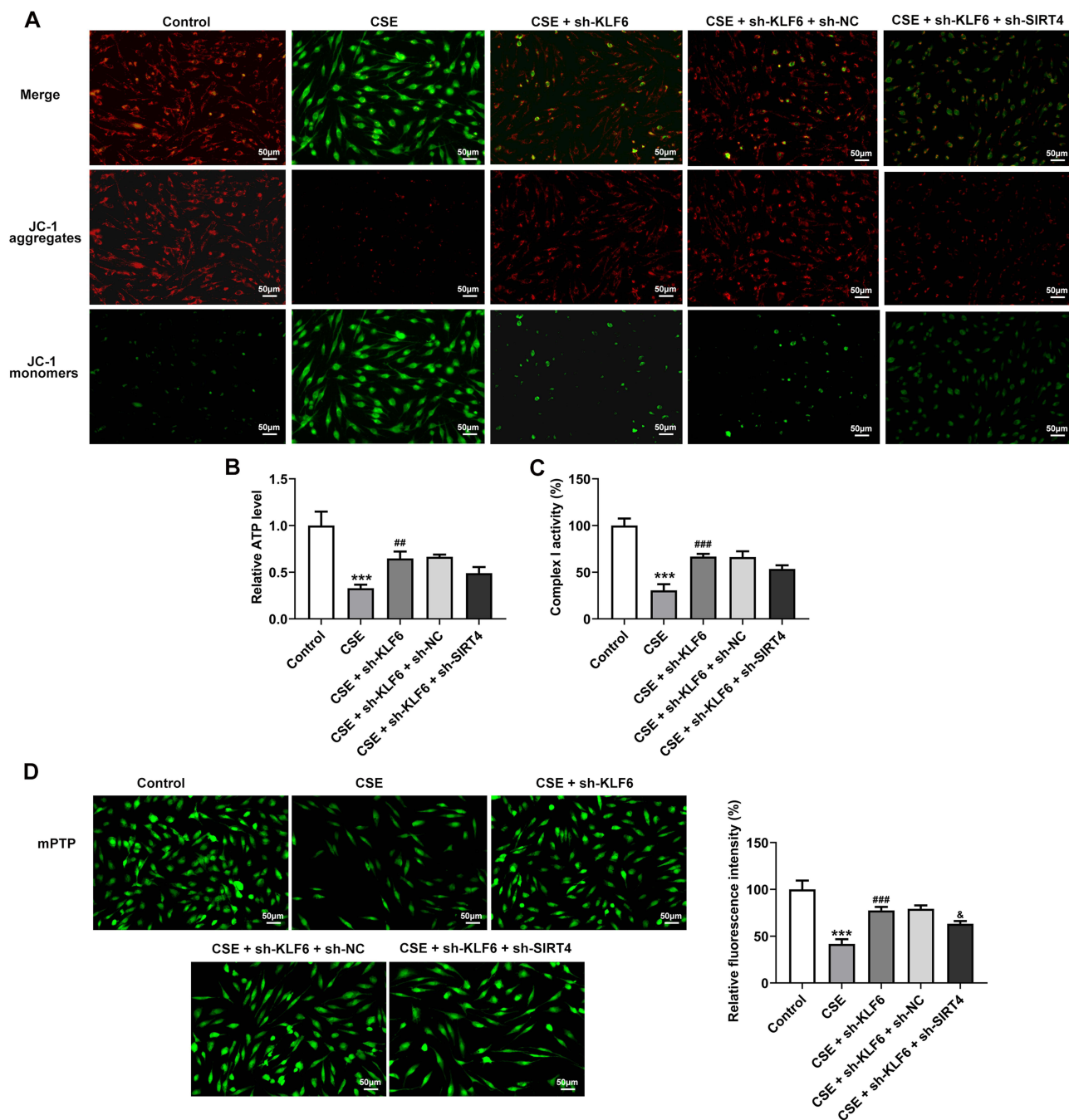


**Figure 7** Inhibition of KLF6 alleviates mitochondrial dysfunction in CSE-induced BEAS-2B cells through SIRT4 upregulation. (A). The MMP was detected by JC-1 fluorescent probe. (B). ATP content was measured with an ATP kit. (C). Complex I activity was detected by the kit. (D). The mPTP opening was tested by the kit. \*\*\* $P < 0.001$  vs Control; ## $P < 0.01$ , ### $P < 0.001$  vs CSE, \* $P < 0.05$  vs CSE+sh-KLF6+sh-NC.

synthesis of ATP can lead to mitochondrial dysfunction.<sup>31</sup> Therefore, in our experiment, we investigated the regulatory effect of KLF6 on mitochondrial function of CSE-induced BEAS-2B cells. We found that the mitochondrial function of BEAS-2B cells was impaired after CSE induction, which was then improved after the interference with KLF6.

JASPAR website predicts the binding sites between KLF6 and SIRT4 promoter. SIRT4 belongs to the type II Sirtuins family and is mainly distributed in mitochondria.<sup>32</sup> Study has shown that the expression of SIRT4 is significantly down-regulated in HPMECs treated with CSE, and SIRT4 negatively regulates CSE-induced NF- $\kappa$ B activation by inhibiting the degradation of I $\kappa$ B $\alpha$  and inhibiting the adhesion of CSE-induced monocytes to HPMECs.<sup>15</sup> Under conditions of high

glucose and high lipid, downregulation of miR-124-3p can induce FOXQ1 in renal tubular epithelial cells, thereby inhibiting SIRT4, leading to mitochondrial dysfunction, and promoting the occurrence of diabetic nephropathy.<sup>33</sup> In our experiments, we found that KLF6 silence could mitigate mitochondrial dysfunction in CSE-induced BEAS-2B cells through SIRT4 upregulation.

## Conclusion

In summary, this study disclosed the role of KLF6 in the viability, apoptosis, inflammation, oxidative stress and mitochondrial dysfunction in CSE-induced BEAS-2B cells and identified that KLF6 inhibited SIRT4 transcription, which for the first time revealed the mechanism by which KLF6 impeded the progression of COPD.

## Disclosure

The authors report no conflicts of interest in this work.

## References

1. Li X, Cao X, Guo M., et al. Trends and risk factors of mortality and disability adjusted life years for chronic respiratory diseases from 1990 to 2017: systematic analysis for the global burden of disease study 2017. *BMJ*. 2020;368:m234. doi:10.1136/bmj.m234
2. Liu X, Ma Y, Luo L, et al. Taxifolin ameliorates cigarette smoke-induced chronic obstructive pulmonary disease via inhibiting inflammation and apoptosis. *Int Immunopharmacol*. 2023;115:109577. doi:10.1016/j.intimp.2022.109577
3. Wang Y, Xia S. Relationship between ACSL4-mediated ferroptosis and chronic obstructive pulmonary disease. *Int J Chron Obstruct Pulmon Dis*. 2023;18:99–111. doi:10.2147/COPD.S391129
4. Do-Umehara HC, Chen C, Zhang Q, et al. Epithelial cell-specific loss of function of Miz1 causes a spontaneous COPD-like phenotype and up-regulates ace2 expression in mice. *Sci Adv*. 2020;6(33):eabb7238. doi:10.1126/sciadv.abb7238
5. Kachuri L, Johansson M, Rashkin SR, et al. Immune-mediated genetic pathways resulting in pulmonary function impairment increase lung cancer susceptibility. *Nat Commun*. 2020;11(1):27. doi:10.1038/s41467-019-13855-2
6. Xu Y, Liu H, Song L. Novel drug delivery systems targeting oxidative stress in chronic obstructive pulmonary disease: a review. *J Nanobiotechnology*. 2020;18(1):145 doi:10.1186/s12951-020-00703-5
7. Li ZY, Zhu Y-X, Chen J-R, et al. The role of KLF transcription factor in the regulation of cancer progression. *Biomed Pharmacother*. 2023;162:114661. doi:10.1016/j.biopha.2023.114661
8. Koritschoner NP, Bocco JL, Panzetta-Dutari GM, et al. A novel human zinc finger protein that interacts with the core promoter element of a TATA box-less gene. *J Biol Chem*. 1997;272(14):9573–9580. doi:10.1074/jbc.272.14.9573
9. Chen Q, Jia Z, Qu C. Inhibition of KLF6 reduces the inflammation and apoptosis of type II alveolar epithelial cells in acute lung injury. *Allergol Immunopathol*. 2022;50(5):138–147. doi:10.15586/aei.v50i5.632
10. Mgbemena V. KLF6 and iNOS regulates apoptosis during respiratory syncytial virus infection. *Cell Immunol*. 2013;283(1–2):1–7 doi:10.1016/j.cellimm.2013.06.002
11. Duan Y, Zhou M, Xiao J, et al. Prediction of key genes and miRNAs responsible for loss of muscle force in patients during an acute exacerbation of chronic obstructive pulmonary disease. *Int J Mol Med*. 2016;38(5):1450–1462. doi:10.3892/ijmm.2016.2761
12. Luo H, Zhou M, Ji K, et al. Expression of sirtuins in the retinal neurons of mice, rats, and humans. *Front Aging Neurosci*. 2017;9:366. doi:10.3389/fnagi.2017.00366
13. Yang Q, Zhou Y, Sun Y, et al. Will sirtuins be promising therapeutic targets for tbi and associated neurodegenerative diseases? *Front Neurosci*. 2020;14:791. doi:10.3389/fnins.2020.00791
14. Dai Y, Liu S, Li J, et al. SIRT4 suppresses the inflammatory response and oxidative stress in osteoarthritis. *Am J Transl Res*. 2020;12(5):1965–1975.
15. Chen Y, Wang H, Luo G, et al. SIRT4 inhibits cigarette smoke extracts-induced mononuclear cell adhesion to human pulmonary microvascular endothelial cells via regulating NF-κB activity. *Toxicol Lett*. 2014;226(3):320–327. doi:10.1016/j.toxlet.2014.02.022
16. Fornes O, Castro-Mondragon JA, Khan A, et al. JASPAR 2020: update of the open-access database of transcription factor binding profiles. *Nucleic Acids Res*. 2020;48(D1):D87–d92. doi:10.1093/nar/gkz1001
17. Dang X, He B, Ning Q, et al. Alantolactone suppresses inflammation, apoptosis and oxidative stress in cigarette smoke-induced human bronchial epithelial cells through activation of Nrf2/HO-1 and inhibition of the NF-κB pathways. *Respir Res*. 2020;21(1):95. doi:10.1186/s12931-020-01358-4
18. Livak KJ, Schmittgen TD. Analysis of relative gene expression data using real-time quantitative PCR and the 2<sup>-</sup>(Delta Delta C(T)) method. *Methods*. 2001;25(4):402–408. doi:10.1006/meth.2001.1262
19. Chung I, Park H-A, Kang J, et al. Neuroprotective effects of ATPase inhibitory factor 1 preventing mitochondrial dysfunction in Parkinson's disease. *Sci Rep*. 2022;12(1):3874. doi:10.1038/s41598-022-07851-8
20. Baker RR. Smoke generation inside a burning cigarette: modifying combustion to develop cigarettes that may be less hazardous to health. *Prog Energy Combust Sci*. 2006;32(4):373–385. doi:10.1016/j.pecs.2006.01.001
21. Crotty Alexander LE, Shin S, Hwang JH. inflammatory diseases of the lung induced by conventional cigarette smoke: a review. *Chest*. 2015;148(5):1307–1322. doi:10.1378/chest.15-0409
22. Zhou L, Jian T, Wan Y, et al. Luteolin alleviates oxidative stress in chronic obstructive pulmonary disease induced by cigarette smoke via modulation of the TRPV1 and CYP2A13/NRF2 signaling pathways. *Int J Mol Sci*. 2023;25(1). doi:10.3390/ijms25010369
23. Pezzuto A, Citarella F, Croghan I, et al. The effects of cigarette smoking extracts on cell cycle and tumor spread: novel evidence. *Future Sci OA*. 2019;5(5):Fso394. doi:10.2144/fsoa-2019-0017

24. Li D, et al., PKM2 regulates cigarette smoke-induced airway inflammation and epithelial-to-mesenchymal transition via modulating PINK1/Parkin-mediated mitophagy, *Toxicology*, 2022;Vol. 477:153251 doi:10.1016/j.tox.2022.153251
25. Li W, Wang J, Hao W, et al. MicroRNA-543-3p down-regulates inflammation and inhibits periodontitis through KLF6. *Biosci Rep*. 2021;41(5). doi:10.1042/BSR20210138
26. Sun J, Cai J, Chen J, et al. Krüppel-like factor 6 silencing prevents oxidative stress and neurological dysfunction following intracerebral hemorrhage via sirtuin 5/Nrf2/HO-1 axis. *Front Aging Neurosci*. 2021;13:646729. doi:10.3389/fnagi.2021.646729
27. Rim Lee Y, Kwon N, Swamy KMK, et al. Rhodamine-thiourea linked naphthalimide derivative to Image ATP in mitochondria using two channels. *Chem Asian J*. 2022;17(15):e202200413. doi:10.1002/asia.202200413
28. Hool LC. Unravelling the mysteries of mitochondria in health and disease. *J Physiol*. 2021;599(14):3447–3448. doi:10.1113/JP281833
29. Jiang Y, Wang X, Hu D. Mitochondrial alterations during oxidative stress in chronic obstructive pulmonary disease. *Int J Chron Obstruct Pulmon Dis*. 2017;12:1153–1162. doi:10.2147/COPD.S130168
30. Yun HR, Jo YH, Kim J, et al. Roles of autophagy in oxidative stress. *Int J Mol Sci*. 2020;21(9):3289. doi:10.3390/ijms21093289
31. Chikuma K, Arima K, Asaba Y, et al. The potential of lipid-polymer nanoparticles as epigenetic and ROS control approaches for COPD. *Free Radic Res*. 2020;54(11–12):829–840. doi:10.1080/10715762.2019.1696965
32. Kumar V, Kundu S, Singh A, et al. Understanding the role of histone deacetylase and their inhibitors in neurodegenerative disorders: current targets and future perspective. *Curr Neuropharmacol*. 2022;20(1):158–178. doi:10.2174/1570159X19666210609160017
33. Liang L, Wo C, Yuan Y, et al. miR -124-3p improves mitochondrial function of renal tubular epithelial cells in db/db mice. *FASEB J*. 2023;37(3): e22794. doi:10.1096/fj.202201202RR

International Journal of Chronic Obstructive Pulmonary Disease

Dovepress

## Publish your work in this journal

The International Journal of COPD is an international, peer-reviewed journal of therapeutics and pharmacology focusing on concise rapid reporting of clinical studies and reviews in COPD. Special focus is given to the pathophysiological processes underlying the disease, intervention programs, patient focused education, and self management protocols. This journal is indexed on PubMed Central, MedLine and CAS. The manuscript management system is completely online and includes a very quick and fair peer-review system, which is all easy to use. Visit <http://www.dovepress.com/testimonials.php> to read real quotes from published authors.

Submit your manuscript here: <https://www.dovepress.com/international-journal-of-chronic-obstructive-pulmonary-disease-journal>